Mohd Ahfaz Khan[1], Dr. Anand Singh[2]

Global MPPT in Solar Photovoltaics: Evaluating PSO, FPA, and CSA Under Partial Shading

Journal of Electrical Systems

Abstract

Maximizing the power output of solar photovoltaic (SPV) systems under partial shading conditions is crucial for improving renewable energy efficiency. Traditional Maximum Power Point Tracking (MPPT) methods often struggle to locate the global Maximum Power Point (MPP) due to multiple local maxima on the power-voltage (P-V) curve. This study evaluates three advanced optimization algorithms—Particle Swarm Optimization (PSO), Flower Pollination Algorithm (FPA), and Cuckoo Search Algorithm (CSA)—to ensure global MPPT under varying environmental conditions. A PV model with three series-connected modules, each containing 20 cells with bypass diodes, is used to mitigate shading effects. Partial shading scenarios involve irradiance levels of 1000 W/m², 300 W/m², and 600 W/m² for the modules, with constant temperature. A DC-DC boost converter extracts maximum power using a 30 mH inductor, 100 µF capacitors, and a 10 kHz switching frequency. PSO adjusts particle positions dynamically, FPA employs Lévy flights for global exploration, and CSA replaces suboptimal solutions to maintain diversity. Performance metrics, including convergence time, tracking efficiency, and precision, are analysed under various irradiance and temperature conditions. Results show that PSO offers rapid convergence, CSA delivers the highest power output with stability, and FPA provides smoother performance but lower efficiency. These findings highlight the trade-offs among these algorithms and their potential for enhancing MPPT in diverse scenarios.

Keywords: Metaheuristic Algorithms, Particle Swarm Optimization, Flower Pollination Algorithm, Cuckoo Search Algorithm, Maximum Power Point Tracking, Partial Shading Conditions, Solar Photovoltaic Systems.

INTRODUCTION

SPV systems have gained significant attention as a renewable energy source due to their environmental benefits and versatility. However, the performance of these systems can be adversely affected by partial shading conditions, which can lead to multiple local maxima in the P-V curves [1]. The traditional MPPT methods, such as perturb and observe (P&O) and incremental conductance (InC), are often unable to locate the global MPP under partial shading conditions [2]. The objectives of the study include evaluating the performance of these metaheuristic

[1]Research Scholar, Electrical & Electronics Department, LNCT University, Bhopal, India
khan.ahfaz@gmail.com[2]Professor, Electrical & Electronics Department, LNCT University, Bhopal, India
anand24883singh@gmail.com

algorithms, analyzing their efficiency, accuracy, and convergence behavior under varying partial shading scenarios, and comparing key performance metrics such as convergence speed, tracking efficiency, computational complexity, and robustness in complex shading conditions.

Additionally, the study aims to highlight the limitations of traditional MPPT methods and demonstrate how PSO, FPA, and CSA overcome these challenges. It seeks to enhance energy harvesting efficiency by accurately tracking the global MPP and provide practical insights for selecting and implementing these algorithms in real-world solar PV systems under different operational and environmental conditions. To address this issue, researchers have proposed various global MPP tracking techniques, including PSO, flower pollination algorithm, and cuckoo search algorithm[3], [4], [5]. This paper aims to evaluate the performance of these three global MPP techniques under partial shading conditions. The literature on MPPT techniques reveals extensive research aimed at addressing the challenges posed by partial shading and dynamic environmental conditions in SPV systems. The evolution of these techniques highlights a progression from traditional methods to advanced optimization algorithms, reflecting the increasing complexity and demands of modern PV systems [6].

Traditional MPPT methods, such as Perturb-and-Observe (P&O) and Hill Climbing, have been widely used due to their simplicity, low computational requirements, and ease of implementation. The P&O method perturbs the PV system's voltage or current and observes the resulting power changes to iteratively locate the MPP. However, it struggles with oscillations around the MPP and fails to converge to the global maximum under partial shading conditions [7]. Similarly, the Hill Climbing method adjusts the operating point in small steps to locate the MPP but is unable to distinguish between local and global maxima, making it suboptimal in complex shading scenarios[8]. Other traditional techniques, such as incremental conductance and fractional open-circuit voltage methods, have attempted to improve tracking efficiency and accuracy but remain limited in handling nonlinearities introduced by partial shading. The limitations of traditional methods have driven the adoption of more sophisticated approaches. Intelligent control-based methods, such as Fuzzy Logic and Artificial Neural Networks, improve adaptability and tracking performance by effectively handling nonlinear P-V curves and dynamic conditions. However, their performance heavily depends on system design, training datasets, and computational resources [9], [10]. Hybrid techniques, which combine traditional methods with intelligent or optimization-based approaches, have also emerged. For example, integrating the incremental conductance method with fuzzy logic enhances tracking precision, while hybrid methods like shuffled frog leaping with incremental conductance improve convergence speed. These techniques, however, involve higher implementation complexity [11].

Metaheuristic algorithms have gained prominence due to their ability to navigate complex search spaces and identify the global MPP under challenging conditions. PSO, inspired by the social behavior of birds and fish, is widely studied for MPPT due to its simplicity and fast convergence. However, its performance may degrade if it becomes trapped in local maxima under severe shading[1], [2]. The FPA, based on the pollination process of flowers, has shown promising results in achieving GMPP, particularly under partial shading. Its ability to balance exploration and exploitation makes it effective for complex optimization problems [12]. Similarly, the CSA, inspired by the brood parasitism of cuckoo birds, is noted for its robustness and convergence efficiency. It has been applied to MPPT with significant success in locating the GMPP while avoiding local maxima [13]. Other algorithms, such as genetic algorithms, ant colony optimization, and simulated annealing, further illustrate the diversity of approaches within the metaheuristic domain. Intelligent control methods offer improved adaptability but require significant computational resources and system tuning. Metaheuristic algorithms consistently outperform other approaches in achieving GMPP under partial shading and dynamic conditions, with trade-offs in computational complexity. The limitations of traditional methods include their inability to distinguish between local and global maxima, slow convergence under dynamic shading conditions, oscillations around the MPP, and limited adaptability to rapidly changing environmental conditions. These challenges underscore the need for advanced optimization algorithms like PSO, FPA, and CSA, which offer promising alternatives for overcoming the limitations of traditional methods and enhancing energy harvesting efficiency.

This study aims to evaluate the effectiveness of PSO, Flower Pollination Algorithm, and CSA in achieving global MPPT under various partial shading scenarios. The performance of these three algorithms under various partial shading scenarios, analyzing their convergence speed, tracking accuracy, and computational efficiency. By leveraging the strengths of PSO, FPA, and CSA, we aim to enhance the reliability and efficiency of MPPT for solar PV systems in diverse environmental conditions. This study is organized into several chapters for clarity and coherence. Chapter III outlines the Methodology employed in this study, describing the photovoltaic (PV) model and system model utilized. It provides a thorough exploration of the optimization algorithms under investigation, including PSO, FPA, and CSA for global MPPT. In Chapter IV, the Results and Discussion section presents the performance analysis of the algorithms across various scenarios, including constant and variable irradiance and temperature conditions. Finally, Chapter V concludes with the References, providing a comprehensive list of sources that informed the study.

I. METHODOLOGY

The methodology investigates the performance of PSO, FPA, and CSA for achieving global MPPT in photovoltaic (PV) systems under partial shading conditions. The study utilizes a single-diode equivalent circuit model of the PV system, incorporating series resistance R_s and shunt resistance R_{sh} to simulate internal losses and leakage currents, respectively. MATLAB/Simulink is employed to model a PV system consisting of three 350 W solar panels connected in series, each equipped with bypass diodes. The PV system is evaluated under four distinct environmental scenarios: constant irradiance and temperature, variable irradiance with constant temperature, constant irradiance with varying temperature, and combined variable irradiance and temperature.

A. PV Model Details

The total 60 solar PV cells are divided into three models and each model has 20 cells. The 20 cell model is rated by following parameter, the open circuit voltage is 12.64 volts, voltage at maximum power is 10.32 volts, short circuit current is 8.62 A and current at MPP is 8.07 and MPP is 83.2824Watts. These three models are connected in series and each model has a bypass diode. The MATLAB/Simulink model of the three series connected solar PV system.

The partial shaded conditions of a solar PV module are created by making irradiance of each at different values such as 1000w/m2 is fixed for panel 1,300 w/m2 for panel 2 and 600 w/m2 for panel 3. And the temperature at each panel is fixed. The power extracted from MPPT is tracking the PSO algorithm. Boost converter is connected between solar PV module and load to extract the maximum power from the partially shaded PV module. The DC-DC boost converter used in this study is designed to enhance the performance of the photovoltaic (PV) system under partial shading conditions. Operating at a 10 kHz switching frequency, the converter features a 30 mH inductor and 100 µF capacitors. It efficiently handles input voltages ranging from 25V to 31V and outputs between 40V and 100V, with a current draw of 2.5A and a maximum voltage ripple of 2V. The converter's design ensures reliable operation, supporting the optimization algorithms in achieving global MPPT.

The PSO algorithm initializes a swarm of particles with random positions and velocities, evaluates their fitness based on the PV system's power output, and updates their positions iteratively using cognitive and social components. This dynamic adaptation enables PSO to converge on the global MPP efficiently. The FPA algorithm employs global pollination using Lévy flights and local pollination through neighborhood interactions. By balancing exploration and exploitation, FPA iteratively updates flower positions to locate the global MPP. Similarly, the CSA algorithm generates new solutions using Lévy flights, discards a fraction of the worst-performing nests, and iteratively updates positions to ensure convergence to the global MPP.

The study evaluates these algorithms across four cases: constant irradiance (1000 W/m²) and temperature (25 °C) for all panels; variable irradiance (1000 W/m², 700 W/m², and 300 W/m²) with constant temperature (25 °C); constant irradiance (1000 W/m²) with varying temperatures (45 °C, 35 °C, and 25 °C); and combined variable irradiance and

temperatures for all panels. The performance of each algorithm is assessed based on convergence time (time taken to locate the global MPP), tracking efficiency (percentage of time accurately tracking the MPP), and tracking precision (accuracy in converging to the global MPP).

The simulation results are analyzed to compare power, voltage, and current characteristics for each algorithm under varying environmental conditions. This systematic evaluation determines the effectiveness of PSO, FPA, and CSA in overcoming local maxima and maximizing power extraction, providing insights into their suitability for dynamic and challenging operating conditions in PV systems.

B. System Model

The single-diode model is a widely accepted representation of a solar cell. It models the solar cell as an ideal current source combined with a diode, along with additional series and parallel resistances to account for losses [14]. This model consists of key components that describe the behavior and efficiency of the cell: Photocurrent Source (I_{ph}) represents the current generated by incident sunlight. The p-n junction of the solar cell, influencing the recombination of charge carriers. Series Resistance (R_s) captures resistive losses caused by material imperfections and internal connections. Shunt Resistance (R_{sh}) is reflects leakage currents across the cell junction, which can reduce efficiency.

The output current (I) of the photovoltaic (PV) cell is expressed mathematically as:

$$I = I_{ph} - c + (V + I.R_s)/R_{sh} - - - - - - - - - - - - (1)$$

In this equation, the output current depends on the photocurrent I_{ph}, diode current I_d, terminal voltage V, and the resistances $R_s\ and\ R_{sh}$. Understanding the Current-Voltage (I-V) and P-V characteristics is essential for evaluating the performance of PV modules, ensuring efficient system design and energy optimization in solar applications.

C. Optimization Algorithms

1. PSO Global MPPT

The flowchart in figure 1 illustrates the implementation of the PSO algorithm for Global MPPT in photovoltaic systems. The process begins with the initialization of the swarm, where particles' positions (x_i) and velocities (v_i) are randomly distributed within the search space. Each particle is also assigned initial personal best (p_{best}) and global best (g_{best}) positions. Subsequently, the fitness of each particle is evaluated based on the power output, calculated as the product of voltage (V) and current (I). Using this fitness value, the personal best (p_{best}) of each particle and the global best (g_{best}) among all particles are updated. The algorithm then proceeds to update the velocity and position of each particle. The velocity is calculated using the equation $v_i^{t+1} = w.v_i^t + c_i.r_i.(p_{best} - x_i^t) + c_2.\ \ r_2.(g_{best} - x_i^t)$, where w represents the inertia weight, c_1 and c_2 are cognitive and social coefficients, and r_1 and r_2 are random numbers between 0 and 1. The position is updated as $x_i^{t+1} = x_i^t + v_i^{t+1}$. The new fitness values are calculated, and the best positions are updated accordingly. A decision block checks whether the stopping criteria are met, which could include reaching the maximum number of iterations or achieving an acceptable error threshold. If the criteria are not satisfied, the algorithm loops back to update velocities and positions. Once the stopping condition is met, the global best position (g_{best}) is output as the MPP, and the corresponding maximum power P_{max} is calculated. The algorithm concludes with the termination step. This systematic flow ensures efficient and accurate tracking of the global MPP under varying environmental conditions. The PSO algorithm's adaptive nature allows it to handle non-linearities and local optima effectively.

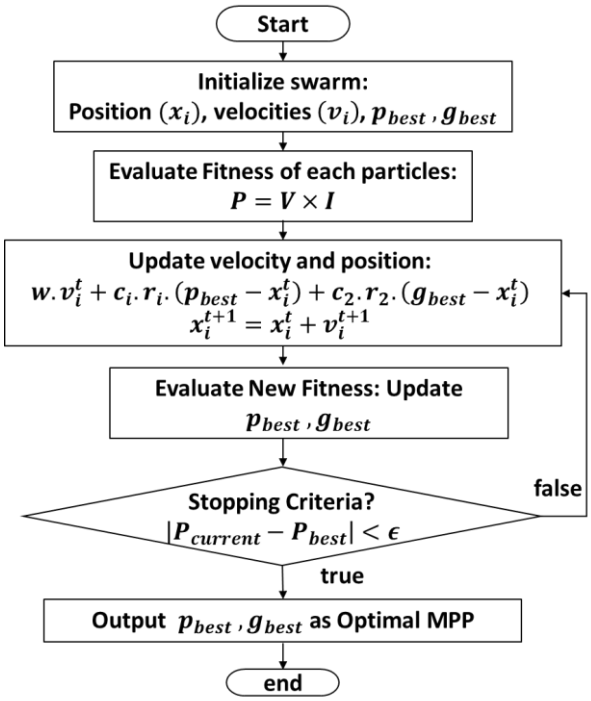

Figure 1: Flowchart for PSO Global MPPT

2. FPA Global MPPT

The flowchart figure 2 represents the implementation of the FPA for achieving global MPPT in photovoltaic (PV) systems. The process begins with the initialization of a population of flowers, where each flower represents a potential solution within the defined search space. The fitness of each flower is evaluated based on its corresponding power output, calculated as $P = V \times I$, ensuring that higher fitness values indicate solutions closer to the MPP.

The global best solution (x_{best}), representing the maximum power output, is identified and used as a reference for guiding the search process. The algorithm employs a probabilistic mechanism to determine whether global or local pollination is performed. In global pollination, Lévy flights are utilized to explore the search space, updating flower positions using the equation $x_i^{t+1} = x_i^t + \lambda L(s)(x_{best} - x_i^t)$ where $L(s)$ represents a Lévy flight distribution. In contrast, local pollination relies on proximity-based adjustments, updating flower positions as $x_i^{t+1} = x_i^t + \epsilon(x_k^t - x_k^t)$, where ϵ is a random scaling factor and x_j , x_k are neighboring flowers.

Following the pollination step, the positions of the flowers are updated, and their fitness values are recalculated, ensuring convergence toward the global MPP. The algorithm checks for stopping criteria, such as reaching a maximum number of iterations or achieving a predefined error threshold $|P_{current} - P_{best}| < \epsilon$. If the criteria are satisfied, the optimal solution (x_{best}) is output, representing the global MPP along with its corresponding maximum power ($P_{max} = V_{MPP}.I_{MPP}$). This systematic approach leverages the global exploration capability of Lévy flights and the local refinement of proximity-based pollination, ensuring efficient and robust tracking of the MPP under varying environmental conditions, including partial shading. As a result, FPA emerges as a powerful tool for enhancing the performance of PV systems.

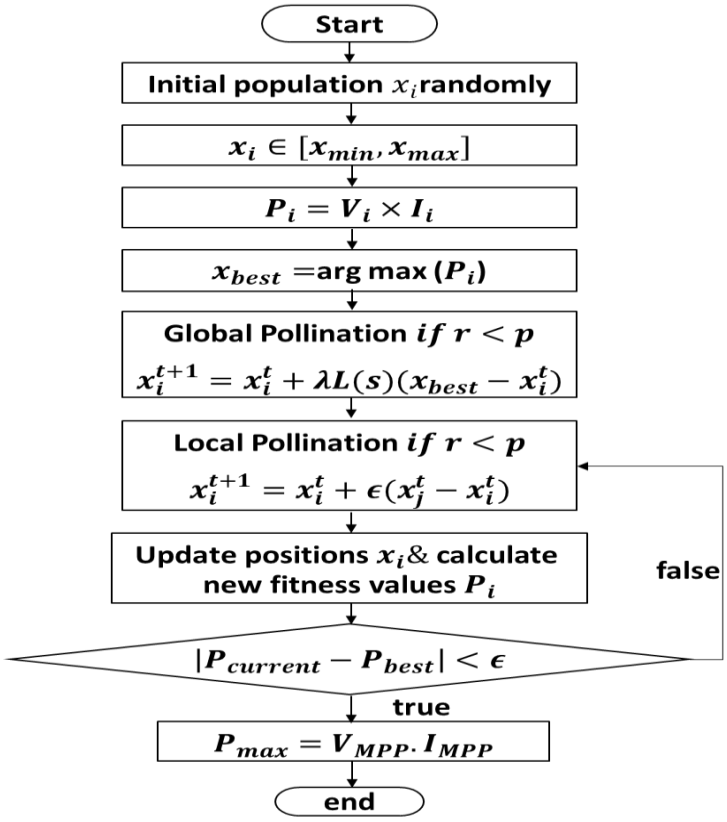

Figure 2: Flowchart for FPA Global MPPT

3. CSA Global MPPT

The flowchart figure 3 illustrates the implementation of the CSA for global MPPT in photovoltaic (PV) systems. The process begins with the initialization of a population of nests, where each nest (x_i) represents a potential solution. The initial positions of the nests are generated randomly within the defined search space. The fitness of each nest is then evaluated based on the power output, calculated as $P = V \times I$. The best nest, representing the highest power output, is identified and stored as the current optimal solution (x_{best}).

In each iteration, new solutions are generated for some nests using Lévy flights, which enable the algorithm to explore the search space effectively. The position update equation is given by $x_i^{t+1} = x_i^t + \alpha L(s)$ where $L(s)$ represents a Lévy flight distribution and α is the step size. To maintain diversity and avoid local optima, a fraction p_a of the worst-performing nests is replaced with new random solutions generated within the search space using $x_i = rand((x_{min}, x_{max})$. After generating the new solutions, the fitness of the updated population is recalculated, and the global best solution is updated if a better nest is found. The algorithm checks the stopping criteria, such as the maximum number of iterations or a predefined error threshold $|P_{current} - P_{best}| < \epsilon$. If the criteria are not met, the process repeats from generating new solutions. Otherwise, the algorithm outputs the global best nest (x_{best}) and its corresponding maximum power output ($P_{max} = V_{MPP}.I_{MPP}$). This systematic approach ensures robust and efficient tracking of the MPP under varying environmental conditions, including partial shading. By leveraging Lévy flights for global exploration and the replacement of weak nests for maintaining diversity, CSA demonstrates its ability to achieve high tracking accuracy, precision, and efficiency in PV systems.

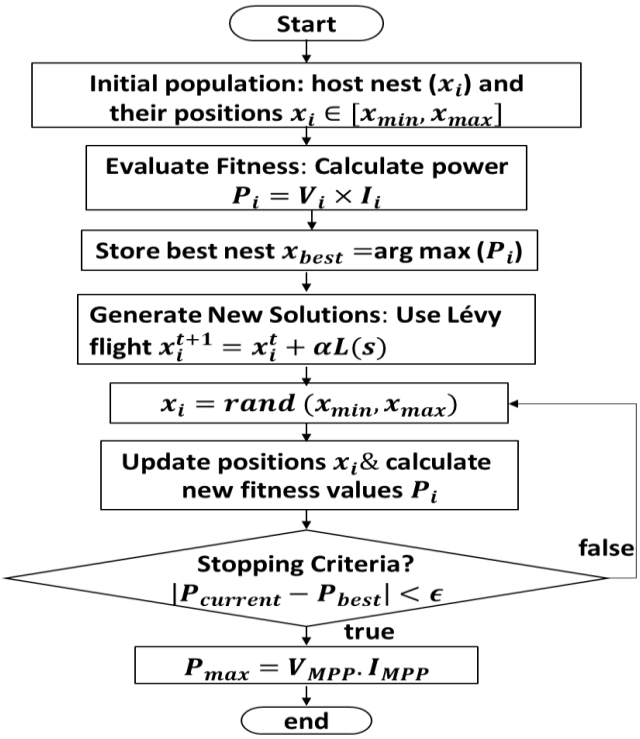

Figure 3: Flowchart for CSA Global MPPT

II. RESULTS AND DISCUSSION

A. Algorithm Performance Analysis

This section presents the results of MATLAB/Simulink simulations for MPPT performance using PSO, FPA, and CSA under various conditions

1. Case I: Constant Irradiance and Temperature

This case examines the performance of three optimization algorithms—PSO, FPA, and CSA—under constant irradiance and temperature conditions, focusing on the time-series characteristics of current, voltage, and power. Figure 4(a) shows that PSO quickly stabilizes the current at approximately 8.8 A within 0.2 seconds, while FPA reaches around 8.5 A with slight oscillations, stabilizing by 0.5 seconds. CSA, on the other hand, stabilizes more slowly at approximately 8.4 A, taking about 1.5 seconds. For voltage, as depicted in Figure 4(b), PSO achieves a steady state of around 100 V after an initial overshoot to 110 V, stabilizing by 0.5 seconds. CSA peaks at 140 V and stabilizes at 120 V with intermediate oscillations by 1.5 seconds, whereas FPA stabilizes at a lower voltage of approximately 30 V with minimal fluctuations. The power output, highlighted in Figure 4(c), shows PSO achieving a steady-state power of ~900 W within 0.2 seconds, while CSA reaches the highest power output, peaking at 950 W and stabilizing at ~930 W by 1.5 seconds. In contrast, FPA stabilizes at a significantly lower power output of ~250 W with negligible oscillations by 0.5 seconds.

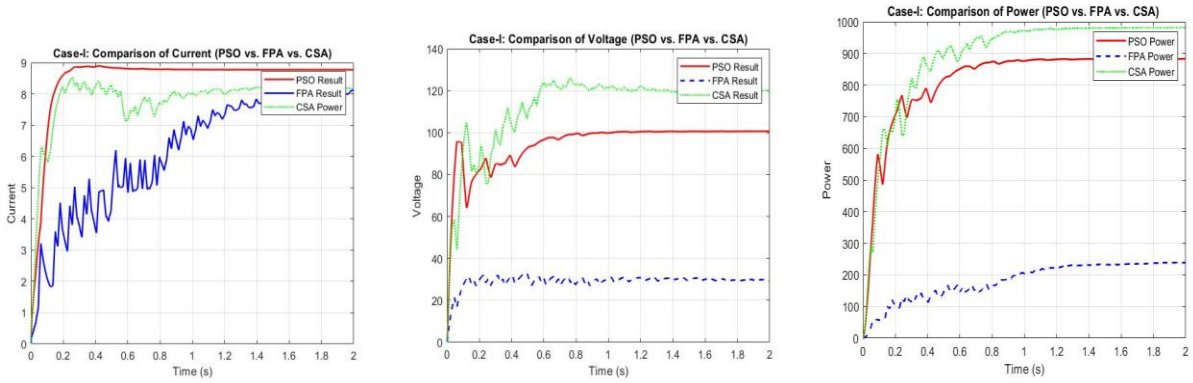

Figure 4(a): Current vs. Time (PSO, FPA, CSA), Figure 4(b): Voltage vs. Time (PSO, FPA, CSA). Figure4(c): Power vs. Time (PSO, FPA, CSA).

Overall, PSO demonstrates rapid convergence with minor oscillations, ensuring high efficiency across current, voltage, and power metrics. FPA offers smooth performance but delivers lower power output. CSA, while slower to converge, achieves the highest power output and maintains stable operation in the long run.

2. Case-II: Variable Irradiance, Constant Temperature

Under variable irradiance and constant temperature conditions, the performance of PSO, FPA, and CSA is compared based on current, voltage, and power outputs. As shown in Figure 5(a), PSO achieves a steady-state current of approximately 8.8 A within 0.2 seconds but experiences significant oscillations, indicating instability. CSA converges more gradually, stabilizing at around 8.4 A by 1.5 seconds with fewer oscillations, reflecting better stability. In contrast, FPA shows the slowest convergence, reaching about 7.5 A with persistent fluctuations, demonstrating lower efficiency in maintaining a stable current. The voltage response, depicted in Figure 5(b), highlights CSA's superior performance, stabilizing at approximately 80 V after 1.5 seconds with minimal fluctuations. PSO stabilizes at around 40 V but suffers from oscillations throughout. FPA, on the other hand, stabilizes at a much lower voltage of approximately 20 V with smoother behavior but suboptimal regulation compared to CSA and PSO. Figure 5(c) presents the power output, where CSA outperforms the other algorithms by achieving the highest peak power of about 450 W and stabilizing with negligible oscillations. PSO delivers moderate power output, stabilizing at around 300 W, but its performance is affected by oscillatory behavior. FPA produces the lowest power output, stabilizing at approximately 150 W with smoother but less effective performance.

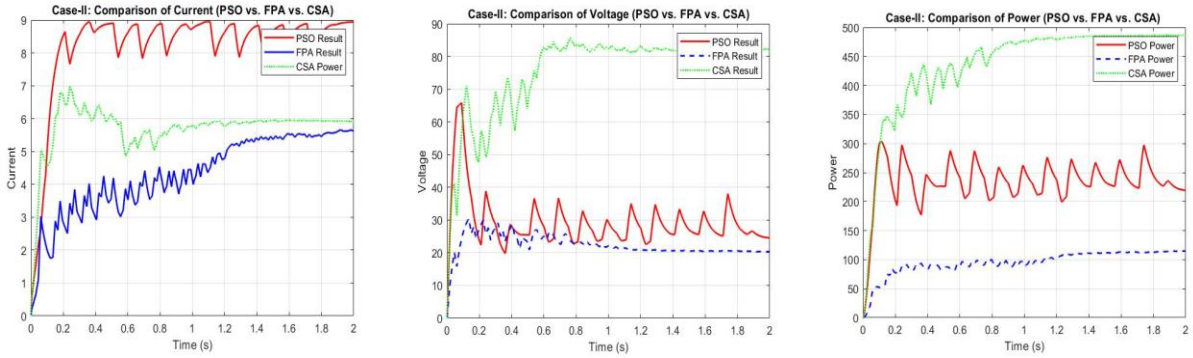

Figure 5(a): Current vs. Time (PSO, FPA, CSA), Figure 5(b): Voltage vs. Time (PSO, FPA, CSA). Figure 5(c): Power vs. Time (PSO, FPA, CSA).

In summary, CSA demonstrates the best overall performance under variable irradiance conditions, achieving the highest current, voltage, and power with stable operation, though it converges more slowly. PSO offers rapid

convergence but suffers from persistent oscillations, which impact its stability. FPA, while smooth and stable, delivers the lowest power output, indicating its inefficiency compared to CSA and PSO.

3. Case-III: Constant Irradiance, Variable Temperature

Under constant irradiance and variable temperature conditions, the performance of PSO, FPA, and CSA is evaluated based on current, voltage, and power outputs. As observed in Figure 6(a), PSO achieves a steady-state current of approximately 9 A within 0.2 seconds, showcasing rapid convergence and stability. CSA converges more gradually, stabilizing at around 8.8 A by 1.5 seconds with fewer oscillations, reflecting better stability than PSO. In contrast, FPA demonstrates slower convergence, reaching a steady-state current of about 8.5 A, but with minor fluctuations, indicating relatively lower efficiency in maintaining a stable current.

The voltage response, shown in Figure 6(b), highlights that CSA stabilizes at approximately 120 V by 1.5 seconds with minimal fluctuations, indicating superior performance. PSO stabilizes at around 100 V but suffers from persistent oscillations throughout the response. Meanwhile, FPA stabilizes at a lower voltage of approximately 80 V, with smoother behavior but suboptimal regulation compared to CSA and PSO.

Figure 6(c) presents the power output, where CSA achieves the highest peak power of approximately 1000 W and stabilizes with negligible oscillations, making it the most effective algorithm under these conditions. PSO delivers moderate power output, stabilizing at around 900 W, although its performance is impacted by oscillatory behavior. FPA produces the lowest power output, stabilizing at approximately 700 W, with smoother but less effective performance.

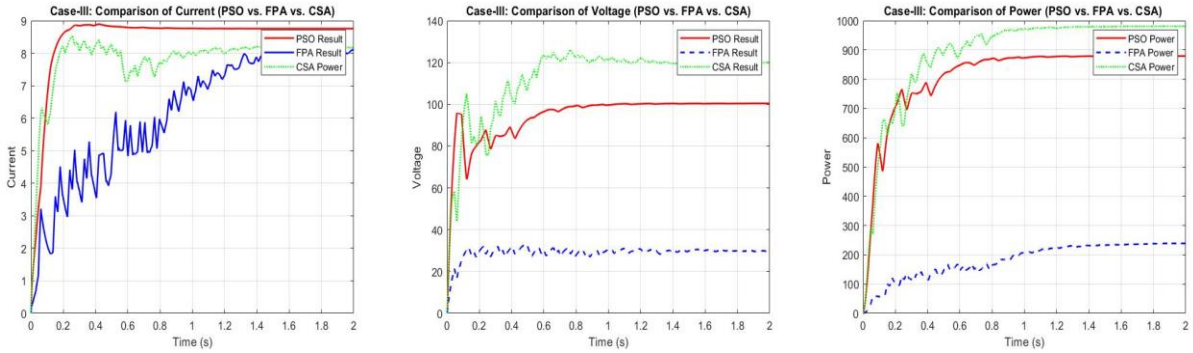

Figure 6(a): Current vs. Time (PSO, FPA, CSA), Figure 6(b): Voltage vs. Time (PSO, FPA, CSA). Figure 6(c): Power vs. Time (PSO, FPA, CSA).

In summary, CSA demonstrates the best overall performance under constant irradiance and variable temperature conditions, achieving the highest current, voltage, and power with stable operation, despite converging more slowly compared to PSO. While PSO offers rapid convergence, it suffers from persistent oscillations, which impact its stability, particularly for voltage and power regulation. FPA, though stable and smooth, delivers the lowest power output, underscoring its inefficiency compared to CSA and PSO.

4. Case-IV: Variable Irradiance and Temperature

Under variable irradiance and temperature conditions, the performance of PSO, FPA, and CSA is analyzed based on current, voltage, and power outputs. As observed in Figure 7(a), PSO achieves a steady-state current of approximately 9 A within 0.2 seconds but exhibits significant oscillations, highlighting its instability. CSA, on the other hand, converges more gradually, stabilizing at around 8.5 A by 1.5 seconds with fewer oscillations, which reflects better stability. In contrast, FPA demonstrates the slowest convergence, stabilizing at about 7.8 A with persistent

fluctuations, indicating lower efficiency in maintaining a stable current. The voltage response, depicted in Figure 7(b), further emphasizes CSA's superior performance as it stabilizes at approximately 85 V after 1.5 seconds with minimal fluctuations. PSO stabilizes at a much lower voltage of around 45 V but is plagued by continuous oscillations throughout the process. FPA, in comparison, stabilizes at about 25 V with smoother behavior but offers suboptimal regulation compared to CSA and PSO. Figure 7(c) reveals the power output, where CSA outperforms both PSO and FPA by achieving the highest peak power of about 480 W and maintaining stability with negligible oscillations. PSO delivers moderate power output, stabilizing at around 310 W, though its performance is compromised by its oscillatory behavior. FPA produces the lowest power output, stabilizing at approximately 200 W with smoother but less effective performance overall.

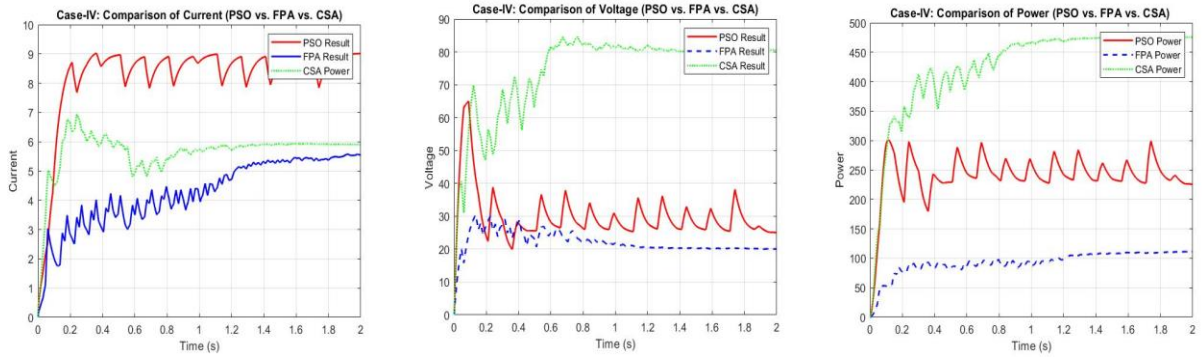

Figure 7(a): Current vs. Time (PSO, FPA, CSA), Figure 7(b): Voltage vs. Time (PSO, FPA, CSA). Figure 7(c): Power vs. Time (PSO, FPA, CSA)

In summary, CSA demonstrates the best overall performance under variable irradiance and temperature conditions, achieving the

5. Comparison of Algorithms

Table 1 compares the performance of PSO, FPA, and CSA across different cases in terms of convergence speed, tracking efficiency, and tracking precision. These comparisons are illustrated by scatter charts in Figures 8(a), 8(b), and 8(c) to provide a visual understanding of the algorithms' behavior.

Table 1: Convergence Speed, Tracking Efficiency, Tracking Precision (%)

Case	Convergence Speed (s)			Tracking Efficiency (%)			Tracking Precision (%)		
	PSO	FPA	CSA	PSO	FPA	CSA	PSO	FPA	CSA
Case I	0.80	1.77	0.97	93.67 %	78.53 %	92.08 %	6.33%	21.47 %	7.92%
Case II	0.10	1.83	1.15	77.78 %	84.14 %	91.14 %	22.22 %	15.86 %	8.86%
Case III	0.80	1.75	0.97	93.96 %	78.55 %	92.14 %	6.04%	21.45 %	7.86%
Case IV	0.10	1.84	1.08	80.59 %	84.58 %	91.00 %	19.41 %	15.42 %	9.00%

Figure 8(a) presents the convergence speed using a chart, highlighting PSO's rapid convergence across all cases. In Case I and Case III, PSO converges in just 0.80 seconds, whereas CSA follows closely with 0.97 seconds. FPA, however, consistently demonstrates the slowest convergence, taking between 1.75 and 1.84 seconds. Notably, in Case II and Case IV, PSO achieves the fastest convergence at an impressive 0.10 seconds, demonstrating its suitability for applications requiring quick responses. Figure 8(b) uses a chart to represent tracking efficiency. CSA achieves the highest tracking efficiency in most cases, particularly in Case II (91.14%) and Case IV (91.00%), reflecting its robust performance. PSO also performs well, with a tracking efficiency of 93.67% in Case I and 93.96% in Case III, slightly surpassing CSA in these scenarios. FPA, on the other hand, lags behind with the lowest efficiency, ranging from 78.53% to 84.58%. Figure 8(c) illustrates tracking precision through a chart, emphasizing CSA's consistent precision across cases. CSA exhibits the lowest tracking errors, with precision values of 7.92% in Case I, 8.86% in Case II, and 7.86% in Case III. PSO, while precise in Cases I and III with values of 6.33% and 6.04%, shows higher tracking errors in Cases II and IV at 22.22% and 19.41%, respectively. FPA demonstrates relatively higher errors, ranging from 15.42% to 21.47%, indicating its limitations in maintaining precise tracking.

Figure 8: PSO, FPA, and CSA Across Different Cases

In summary, Figures 8(a), 8(b), and 8(c) collectively demonstrate the performance trade-offs among PSO, FPA, and CSA. PSO excels in convergence speed but occasionally struggles with precision. CSA balances speed, efficiency, and precision, making it the most consistent performer. In contrast, FPA lags in all metrics, underscoring its lower suitability for dynamic conditions. These visualizations reinforce the conclusion that CSA provides the most reliable performance for MPPT under varying conditions.

III. CONCLUSION

This study systematically evaluates the effectiveness of PSO, FPA and CSA in achieving global MPPT under various partial shading conditions in photovoltaic systems. Each algorithm demonstrated unique strengths and limitations across the four tested scenarios: constant irradiance and temperature, variable irradiance with constant temperature, constant irradiance with variable temperature, and combined variable irradiance and temperature. PSO exhibited rapid convergence and effective tracking performance, making it well-suited for applications requiring quick responses. However, its tendency to oscillate and occasionally converge to local maxima under dynamic conditions highlights the need for further refinement in its implementation. FPA, while delivering smoother performance with minimal

oscillations, showed the lowest tracking efficiency and power output, indicating room for improvement in its optimization capabilities under diverse scenarios. CSA emerged as the most robust and consistent algorithm, achieving the highest power output and tracking efficiency with stable operation, though it converges more slowly than PSO.

The results emphasize the importance of selecting the right optimization algorithm based on specific operational requirements and environmental conditions. While PSO offers speed, CSA ensures stability and precision, and FPA provides smoother transitions. Together, these findings underscore the potential of advanced metaheuristic algorithms to significantly enhance MPPT strategies, contributing to more efficient energy harvesting in SPV systems.

Future research may focus on hybridizing these algorithms to combine their individual strengths and further optimize their performance. Additionally, practical implementation and hardware validation will help bridge the gap between simulation results and real-world applications, ensuring broader adoption in renewable energy systems.

IV. REFERENCES

[1] A. A. Zaki Diab and H. Rezk, "Global MPPT based on flower pollination and differential evolution algorithms to mitigate partial shading in building integrated PV system," *Sol. Energy*, vol. 157, pp. 171–186, Nov. 2017, doi: 10.1016/j.solener.2017.08.024.

[2] N. Sy, C.-S. Chiu, and W.-E. Shao, "MPPT Design for a DC Stand-Alone Solar Power System with Partial Shaded PV Modules," in *2019 International Conference on System Science and Engineering (ICSSE)*, Dong Hoi, Vietnam: IEEE, Jul. 2019, pp. 31–36. doi: 10.1109/ICSSE.2019.8823469.

[3] F. Belhachat and C. Larbes, "A review of global maximum power point tracking techniques of photovoltaic system under partial shading conditions," *Renew. Sustain. Energy Rev.*, vol. 92, pp. 513–553, Sep. 2018, doi: 10.1016/j.rser.2018.04.094.

[4] M. A. M. Ramli, S. Twaha, K. Ishaque, and Y. A. Al-Turki, "A review on maximum power point tracking for photovoltaic systems with and without shading conditions," *Renew. Sustain. Energy Rev.*, vol. 67, pp. 144–159, Jan. 2017, doi: 10.1016/j.rser.2016.09.013.

[5] A. A. Zaki Diab and H. Rezk, "Global MPPT based on flower pollination and differential evolution algorithms to mitigate partial shading in building integrated PV system," *Sol. Energy*, vol. 157, pp. 171–186, Nov. 2017, doi: 10.1016/j.solener.2017.08.024.

[6] M. Seyedmahmoudian *et al.*, "A Sustainable Distributed Building Integrated Photo-Voltaic System Architecture with a Single Radial Movement Optimization Based MPPT Controller," *Sustainability*, vol. 12, no. 16, p. 6687, Aug. 2020, doi: 10.3390/su12166687.

[7] A. N. Mahmod Mohammad, M. A. Mohd Radzi, N. Azis, S. Shafie, and M. A. Atiqi Mohd Zainuri, "An Enhanced Adaptive Perturb and Observe Technique for Efficient Maximum Power Point Tracking Under Partial Shading Conditions," *Appl. Sci.*, vol. 10, no. 11, p. 3912, Jun. 2020, doi: 10.3390/app10113912.

[8] A. Jawad Khadhim Alrubaie, M. Faridun Naim Tajuddin, T. Eddine Khalil Zidane, and A. Azmi, "Improved hill climbing algorithm with fast scanning technique under dynamic irradiance conditions in photovoltaic system," *J. Phys. Conf. Ser.*, vol. 1432, no. 1, p. 012061, Jan. 2020, doi: 10.1088/1742-6596/1432/1/012061.

[9] A. M. Noman, K. E. Addoweesh, and A. I. Alolah, "Simulation and Practical Implementation of ANFIS-Based MPPT Method for PV Applications Using Isolated Ćuk Converter," *Int. J. Photoenergy*, vol. 2017, pp. 1–15, 2017, doi: 10.1155/2017/3106734.

[10] Woonki Na, Pengyuan Chen, Jonghoon Kim, and Hong-Ju Jung, "Improved maximum power point tracking algorithm using a Fuzzy Logic Controller for a Photovoltaic System," in *2016 IEEE 7th International Symposium on Power Electronics for Distributed Generation Systems (PEDG)*, Vancouver, BC, Canada: IEEE, Jun. 2016, pp. 1–5. doi: 10.1109/PEDG.2016.7527033.

[11] P.-Y. Chen, K.-N. Yu, H.-T. Yau, J.-T. Li, and C.-K. Liao, "A novel variable step size fractional order incremental conductance algorithm to maximize power tracking of fuel cells," *Appl. Math. Model.*, vol. 45, pp. 1067–1075, May 2017, doi: 10.1016/j.apm.2017.01.026.

[12] J. Prasanth Ram and N. Rajasekar, "A Novel Flower Pollination Based Global Maximum Power Point Method for Solar Maximum Power Point Tracking," *IEEE Trans. Power Electron.*, vol. 32, no. 11, pp. 8486–8499, Nov. 2017, doi: 10.1109/TPEL.2016.2645449.

[13] I. Ferdiansyah, S. Sutedjo, O. A. Qudsi, and A. Noer Ramadhan, "Implementation of Maximum Power Point Tracking on Solar Panels using Cuckoo Search Algorithm Method," in *2019 2nd International Conference on Applied Information Technology and Innovation (ICAITI)*, Denpasar, Bali, Indonesia: IEEE, Sep. 2019, pp. 88–92. doi: 10.1109/ICAITI48442.2019.8982163.

[14] Vinod, R. Kumar, and S. K. Singh, "Solar photovoltaic modeling and simulation: As a renewable energy solution," *Energy Rep.*, vol. 4, pp. 701–712, Nov. 2018, doi: 10.1016/j.egyr.2018.09.008.